LAWRENCE
LIVERMORE
NATIONAL
LABORATORY

LLNL-PROC-422695

3D Simulations of the NIF Indirect Drive Ignition Target Design

O. S. Jones, J. L. Milovich, D. A. Callahan, M. J. Edwards, O. L. Landen, J. D. Salmonson, D. S. Clark, S. W. Haan, M. M. Marinak, M. V. Patel, S. H. Langer, S. M. Sepke, P. T. Springer, S. P. Hatchett

January 21, 2010

IFSA Conference
San Francisco, CA, United States
September 6, 2009 through September 11, 2009

Disclaimer

3D Simulations of the NIF Indirect Drive Ignition Target Design

O.S. Jones, J.L. Milovich, D.A. Callahan, M.J. Edwards, O.L. Landen, J.D. Salmonson, D.S. Clark, S.W. Haan, M.M. Marinak, M.V. Patel, S.H. Langer, S.M. Sepke, P.T. Springer, S.P. Hatchett

Lawrence Livermore National Laboratory, P.O. Box 808, Livermore, CA 94551, USA

Email: jones96@llnl.gov

Abstract. The radiation hydrodynamics code Hydra is used to quantify the sensitivity of different NIF ignition point designs to several 3D effects. Each of the 48 NIF quads is included in the calculations and is allowed to have different power. With this model we studied the effect on imploded core symmetry of discrete laser spots (as opposed to idealized azimuthally-averaged rings) and random variations in laser power.

1. Introduction

Historically, most of the design work to specify the combination of hohlraum dimensions, materials, and laser power and pointing that delivers the desired radiation drive for a given ICF capsule has been done using axi-symmetric calculations. Calculations that assume axial symmetry have generally been found to give good agreement with many hohlraum experiments done on laser facilities such as Omega. However, the very tight tolerances on implosion symmetry that are required for an ignition target mean that nonideal 3D effects need to be included in more detailed calculations in order to assess the sensitivity of a particular design to these effects.

To do these calculations, we used the radiation hydrodynamics code Hydra [1]. Approximately 30 million census photons were used for the implicit Monte Carlo radiation transport. The capsule and hohlraum materials were divided up into about 2 million computational zones. The capsule angular zoning is 2.5 degrees in the polar direction and 4.5 degrees in the azimuthal direction. This type of zoning is adequate for resolving low modes (up to mode 8) that characterize the radiation drive asymmetry. Effects of higher mode perturbations due to capsule and fuel surface roughness are not included in this type of calculation. The thin plastic window across the laser entrance hole (LEH) that holds in the hohlraum fill gas is included, as are the different layers of wall material (typically gold, gold/boron, and uranium). The wall material in the calculations is 50 microns thick at the barrel and 100 microns thick at the LEH insert. This is thicker than the actual thicknesses of the hohlraum (30 microns at the barrel and 50 microns at the LEH insert). The thicker wall was needed to accommodate the zoning strategy employed near the LEH, which required that the outer boundary of the wall to be fixed

We define ignition time for an igniting capsule as the time at which the central temperature exceeds 12 keV. At that time, we define the local hotspot radius as the radius at which the density along any ray emanating from the center equals half of the maximum density along that ray. Since the hotspot surface can be expressed in terms of the spherical harmonics, Y_{lm}, then the rms deviation of the hotspot from its average value can be expressed in terms of the coefficients of the spherical harmonics, a_{lm}. The expression for the hotspot rms is given by

$$\xi = \sqrt{\frac{\iint (r - R_{avg}) d\Omega}{4\pi}} \frac{1}{R_{avg}} = \sqrt{\sum\sum\left(\frac{a_{lm}}{a_{00}}\right)^2} . \qquad (1)$$

The m=0 spherical harmonic are the axisymmetric modes, and the Y_{l0} functions are proportional to the more familiar Legendre polynomials (P_2, P_4, etc.).

2. Calculating the intrinsic 3D radiation asymmetry

The NIF laser consists of 192 laser beams grouped into 48 quads of beams. The quads are grouped into 4 cones per side at polar angles of 23.5, 30, 44.5, and 50 degrees. The beams are pointed such that the 23.5 and 30 degree cones ("inner cones") illuminate the hohlraum near the midplane and the

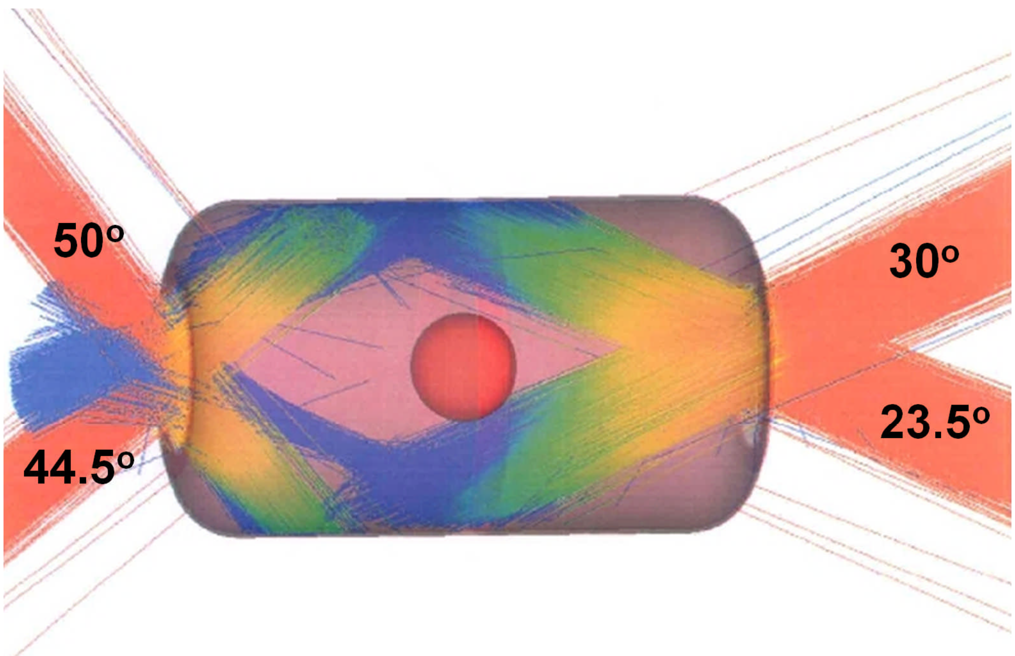

Figure 1. Material boundary plot from 3D calculation showing one quad at each polar angle.

44.5 and 50 degree cones ("outer cones") illuminate the hohlraum wall farther out toward the LEH, as shown in Figure 1. There are 4 quads per side for the 23.5 and 30 degree cones and 8 quads per side for the 44.5 and 50 degree cones. To control the lowest even Legendre mode asymmetry (P_2), a different laser power versus time is used for the inner and outer cones. The P_4 asymmetry is controlled by varying the hohlraum length to change the polar angle of the outer ring of beams relative to the capsule. Each NIF quad is treated as a single f/8 beam.

(a) (b) (c)

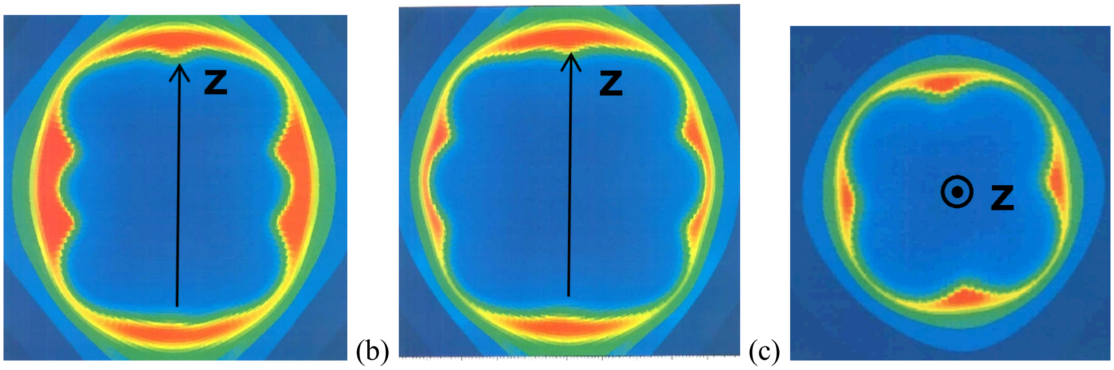

Figure 2. Density slices at maximum compression, (a) ϕ=0 , (b) ϕ=90, (c) z=0

The amount of intrinsic 3D radiation drive asymmetry due to the 3D illumination pattern was investigated for a 1180 micron radius doped beryllium ablator capsule driven with a peak radiation drive of 285 eV [2]. The pointing and inner/outer cone balance were adjusted so that an axisymmetric calculation gave a symmetric implosion. Then the same parameters were used for an ideal (no random errors in pointing or power) 3D calculation. Figure 2 shows contours of density at the time of maximum compression. Slices in the ϕ=0 and ϕ=90 degree planes show the Y40 asymmetry, and a slice across the midplane clearly shows an m=4 asymmetry. The m=4 is caused by the variation in brightness between 23.5 and 30 degree beams. This core has a total hotspot rms of 9.6%. There is 6.4% from a_{20}, 3.7% from a_{40}, 2.8% from a_{44}, and 1.4% from a_{54}. So the m=4 modes contribute about 3% to the total rms asymmetry.

3. Effect of laser power balance on core shape

The sensitivity to laser power balance was assessed for a 1000 micron radius Be capsule driven with a peak radiation drive temperature of 300 eV [3]. The power balance was estimated from a sequence of 16 full power single beam shots on NIF. The shot-to-shot differences in laser power were due to variations in the power and energy injected into the main laser, differences in amplifier gain, and differences in crystal detuning angle. Figure 3 shows the fractional difference in the laser power for each shot relative to the power of the average shot in the 16 shot sequence. Also shown is the rms variation of the 2-ns-averaged pulses as compared to the NIF specification.

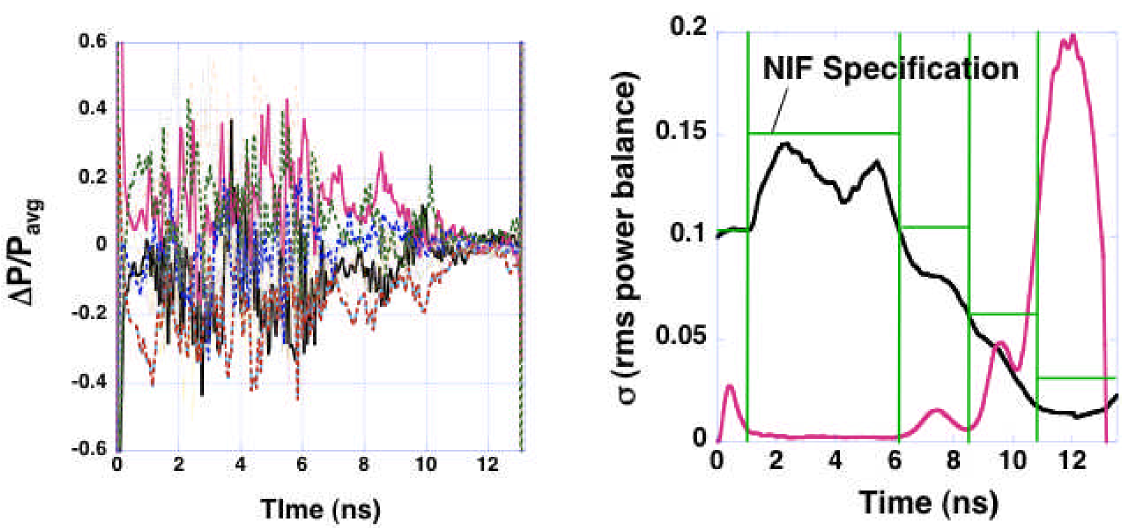

Figure 3. Fractional deviation in power from average for 16 sequential single beam NIF shots

Each measured power difference was multiplied by two small random numbers to create 32 more statistically equivalent traces. The difference in power was then mapped onto a laser pulse shape tuned numerically for the 285 eV Be ablator design. The same 48 power traces were used for all runs, with different random realizations accomplished by assigning a particular quad a different power trace each run. Figure 4 shows the contribution of laser power balance to the hotspot rms as a function of a power balance multiplier. The net contribution due to power imbalance is obtained for each case by subtracting the hotspot rms for a baseline case with perfect power balance. We concluded that the measured power imbalance contributed about 0.1 to the hotspot rms.

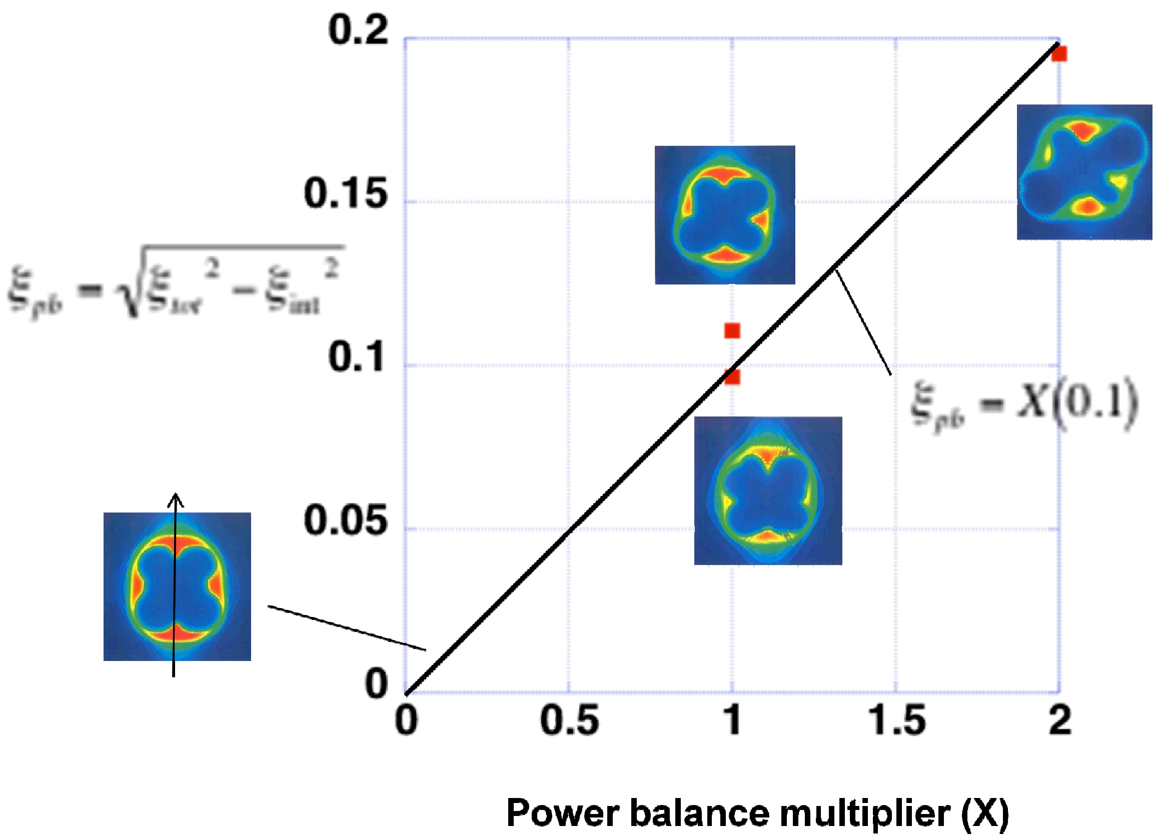

Figure 4. Sensitivity of hot spot rms to power balance multiplier for 285 eV Be ablator design

4. Conclusions

The Hydra radiation code was used to determine the sensitivity of NIF point designs to 3D effects. The radiation asymmetry due to the intrinsic 3D illumination pattern contributed about 0.03 to the final imploded core hotspot rms. The amount of laser power imbalance inferred from NIF measurements contributes 0.1 to the hotspot rms.

References

[1] M. M. Marinak, et al., *Phys. of Plasmas*, **8**, *5*, 2275 (2001)

[2] J. D. Salmonson, et al., Bull. Am. Phys. Soc., **52**, 273 (2007)

[3] S. W. Haan, et al., Fusion Sci. and Technol., **51**, 509 (2007)

This work performed under the auspices of the U.S. Department of Energy by Lawrence Livermore National Laboratory under Contract DE-AC52-07NA27344.